

## Influence of Grain Boundary Phase Transitions on the Properties of Cu-Bi Polycrystals

B.B.Straumal<sup>1,3</sup>, N.E.Sluchanko<sup>2</sup> and W.Gust<sup>3</sup>

<sup>1</sup>Institute of Solid State Physics, Russian Academy of Sciences,  
142432 Chernogolovka, Russia

<sup>2</sup>General Physics Institute, Russian Academy of Sciences,  
Vavilova str. 38, 117942 Moscow, Russia

<sup>3</sup>Max-Planck Institute for Metals Research and Institute of Physical Metallurgy,  
Seestrasse 92, 70174 Stuttgart, Germany

e-mail: straumal@song.ru

**Keywords:** Grain Boundaries, Phase Transitions, Cu-Bi System

**Abstract.** The grain boundary (GB) properties depend hardly on the GB phase transitions. The GB wetting phase transitions in the two-phase area of the bulk phase diagram control the penetration of a liquid phase along GBs. The GB prewetting and/or premelting phase transitions in the one-phase area of the bulk phase diagram where only the solid solution is in equilibrium lead to the formation of an equilibrium layer of a GB phase having a high diffusivity. New method for the investigation of GB phase transition in polycrystals is proposed namely the low-temperature resistivity measurements. The sudden changes of residual resistivity, temperature derivative of the resistivity and GB segregation in the Cu-Bi coincide and reveal the GB prewetting phase transition in the solid solution area of the Cu-Bi phase diagram. The presence of a quasi-liquid layer at GBs can explain the enhanced GB diffusivity in the Cu-Bi system, similar to that observed earlier in the Fe-Si-Zn system.

### Introduction

Encouraged by the success in the investigations of the phase transitions on the free surfaces [1-3], the search on the grain boundary (GB) phase transitions was started in the 80-es. Big efforts in this area resulted in new knowledge in this important branch of physics and materials science. The GB phase transitions can be divided into two main groups.

(1) *Structural GB phase transitions.* These GB phase transitions can proceed in pure one-component materials. They are determined mainly by the energetic and geometric pattern in the GB plane defined by the crystallographic structure and misorientation of both grains. These GB phase transitions are rather insensitive to the kind of material and even to the concentration of the second component [4]. A good examples of such phenomena are the "special GB – general GB" phase transitions proceeding close to the so-called coincidence misorientations  $\theta_{\Sigma}$  [4-7]. By changing the misorientation angle  $\theta$  and increasing  $\Delta\theta = |\theta_{\Sigma} - \theta|$  the GBs loose their special structure and properties and transform into general ones. If  $\Sigma$  is not too low, the special GBs can loose their special structure and properties not only by increasing  $\Delta\theta$  but also by increasing temperature [6, 7]. In other words, the energetic minimum at  $\theta_{\Sigma}$  disappears at increasing temperature. Another example of the structural GB phase transitions is the *GB faceting* [8, 9]. If the mutual misorientation of the grains is fixed, the GB still have two degrees of freedom defining its orientation (inclination). Certain inclinations  $\phi$  correspond to the energetic minima. The GB having an intermediate inclination has a higher energy and tends to "dissolve" into two phases – GB facets of lower energy.

(2) *"Chemical" GB phase transitions.* For these transitions the presence of the second (or third etc.) component is essential. Such GB phase transitions can be described using the additional GB lines in the conventional bulk phase diagrams. The position of these GB lines is rather insensitive to the crystallography of GBs. In case of "chemical" phase transitions the pure GB is replaced by the layer of the second phase. Two main situations are possible. In the first case *at least two bulk phases  $\alpha$  and  $\beta$  are in the equilibrium.* If the energy  $\gamma_{\alpha\alpha}$  of the GB in the phase  $\alpha$  is lower than the

energy  $2\gamma_{\alpha\beta}$  of two interphase boundaries  $\alpha/\beta$ , a layer of the  $\beta$ -phase has to separate two  $\alpha$ -grains one from another replacing the  $\alpha/\alpha$  GB. If the  $\beta$ -phase is liquid, such a process is called the GB wetting phase transition. The GB phase transition from the incompletely to completely wetted GB can proceed both by changing temperature and concentration. Such transitions are studied experimentally and well documented for many two and three-component systems [10–18]. The thermodynamics allows that a stable thin layer of a phase can exist on the GB even if only one phase is stable in the bulk. Such a layer can suddenly appear on the GB as a result of the GB premelting or prewetting phase transition [19, 20]. The model of the GB premelting or prewetting phase transition allowed to explain the extremely high rate of interface and GB diffusion [15–17, 21, 22], the abnormal increase of the GB mobility with increasing impurity content [23], the anomalous GB segregation [24–26], and the presence of a stable thin layer of the second phase in GBs [20].

Unfortunately, the measurements of GB diffusion permeability or GB segregation as methods for the investigation of GB phase transitions are rather complicated and have some restrictions. Particularly, the GB segregation can only be measured in the systems possessing GB brittleness like the Cu–Bi alloys. The GB diffusivity cannot be measured at low and high temperatures. At low temperature the GB penetration profiles is too shallow to be measured. At high temperature the GB penetration depth is comparable with the bulk one, and the GB input into overall diffusion permeability is hard to distinguish from the bulk input. Therefore, the new methods for the investigation of GB phase transitions complementary to the existing ones have to be developed. In this work the GB segregation in the Cu–Bi diluted alloys and the low-temperature resistivity of these polycrystals are measured.

### Experimental

Cylindrical Cu(Bi) polycrystals containing  $x_{Bi}^v = 25, 50$  and  $75$  at. ppm Bi were produced from Cu and Bi of 99.999 at. % purity by casting in vacuum. All samples were homogenized for 24 h at 1273 K in evacuated ( $5 \times 10^{-4}$  Pa) silica ampoules. After homogenization, the Bi content in the specimens was measured by atom absorption spectroscopy in a Perkin-Elmer spectrometer (model 5000). The specimens were then annealed at temperatures  $T_{an}$  between 773 and 1273 K for various times estimated from the Bi diffusion coefficient in Cu. The details of the heat treatment conditions are given in [27]. After annealing the specimens were quenched *ex-situ* and then fractured *in-situ* in the ultra high vacuum chamber of the PHI 600 Scanning Auger Multiprobe at the temperature of liquid nitrogen. The Bi concentration was measured by means of the Auger electron spectroscopy (AES) at 20–30 sites on the fracture surface. The standard methods of the Auger signal processing have been used [27]. In this work we express the Gibbsian excess of Bi atoms at the GBs in monolayers (ML) of Bi. One ML of pure Bi contains  $9.3$  atoms/nm<sup>2</sup>.

The samples of size  $3 \text{ mm} \times 7 \text{ mm} \times 0.3 \text{ mm}$  for the low-temperature resistivity measurements were cut by spark erosion. Afterwards the samples were chemically thinned to the thickness about 0.1 mm in the H<sub>2</sub>NO<sub>3</sub> 50% water solution. The measurements of the temperature dependence of the resistivity of Cu–Bi polycrystals were made with the aid of the experimental installation which consists of: (a) various cryogenic assemblies; (b) systems for the measurements of the low and high temperature; (c) systems for the sample positioning; (d) various magnet systems and (e) system for helium gas handling. Data acquisition was performed through the interface RS-232 by the original microprocessor device controlled by the IBM PC. Universal insert equipped with various exchangeable parts for the work in different temperature intervals and media (like vacuum, inert gases and cryogenic liquids) was used for the measurements. The construction includes: (a) thermo-isolation unit for conduction of measurements in various thermal regimes; (b) circuits for operation in various helium gas-liquid flow regimes; (c) exchangeable cups and measurement cells with temperature sensors and additional heaters.

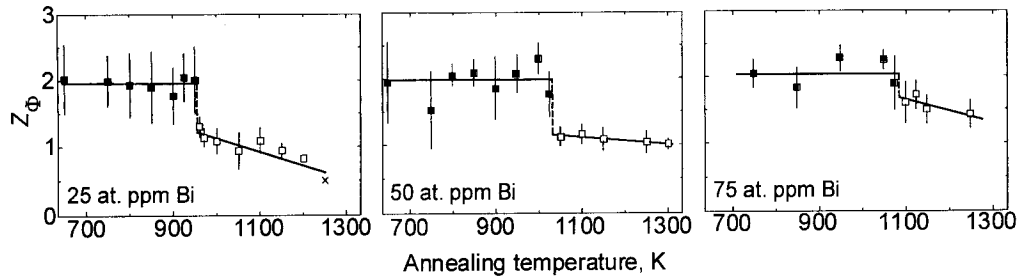


Fig. 1. Temperature dependence of the GB Gibbsian excess of Bi in Cu(Bi) polycrystals of various compositions, measured by AES.

The sample was mounted in the measurement cell which fixed in the insert by the screw fixator. The measurement cell and the screen were made of copper having high thermal conductivity. It permits to diminish the thermal gradients in the working volume and to exclude the possible negative influence of the thermopower. In order to ensure the electric isolation and to keep in the same time the good thermal contact, the sample was glued in the cell to the sapphire substrate having the thickness of 0.1 to 0.25 mm. The contact wires were made of copper coated with silver. The reliable contact of these wires to the sample was ensured by the soldering or spark welding.

Measurements of the resistivity of Cu–Bi polycrystals were performed in the direct current regime from 4.2 to 300 K. The cooling of the insert with the measurement cell were performed by the vapor of liquid helium in the Dewar vessel STG-40 or in the cryogenic assembly. For the temperature measurements the carbon resistivity thermometer TVO ( $R_{273K} = 2.7 \text{ k}\Omega$ ) was used. It was calibrated by the standard resistivity thermometer TSU-2 in the temperature interval from 1.75 to 300 K. Usage of the low measurement current of  $10 \mu\text{A}$  in the temperature interval from 20 to 300 K and  $1 \mu\text{A}$  in the temperature interval from 1.75 to 20 K permitted to exclude possible measurement error due to the heating of the thermosensor. The error of the temperature measurements was about 0.1 to 0.3 K above 100 K and decreased down to 0.01 K below 100 K.

## Results

In Fig. 1 the temperature dependence of the GB Gibbsian excess  $Z^\Phi$  of Bi in Cu–Bi polycrystals is shown. The step-like discontinuous decrease of the  $Z^\Phi$  value can be clearly seen. The cross for  $x_{Bi}^v = 25 \text{ at. ppm Bi}$  is used for the samples which exhibited a ductile fracture and on which, therefore, it was impossible to perform the AES measurements. At higher concentrations ( $x_{Bi}^v = 50$  and  $75 \text{ at. ppm Bi}$ ) the step-like discontinuous decrease of the  $Z^\Phi$  value is more pronounced and appears at higher temperatures. At temperatures below the jump, the Gibbsian excess  $Z^\Phi$  in polycrystals is constant and rather high reaching 2 ML. At temperatures above the  $Z^\Phi$  jump, the usual GB segregation was observed in polycrystals, the  $Z^\Phi$  value was about 1 ML and decreased with increasing temperature. In order to visualize the discontinuous nature of the GB segregation transition we used filled and open symbols in Fig. 1 for the high- and low-Bi content branches of the respective temperature dependences.

Fig. 2 represents the temperature dependence of the resistivity  $\rho$  of the Cu – 75 at. ppm Bi polycrystals annealed at various temperatures  $T_{an}$  and subsequently quenched. The value of  $\rho$  increases monotonously with increasing temperature of measurements  $T$ . Above  $\sim 100 \text{ K}$   $\rho$  depends linearly on  $T$ . Two values were extracted from each curve, namely the residual resistivity

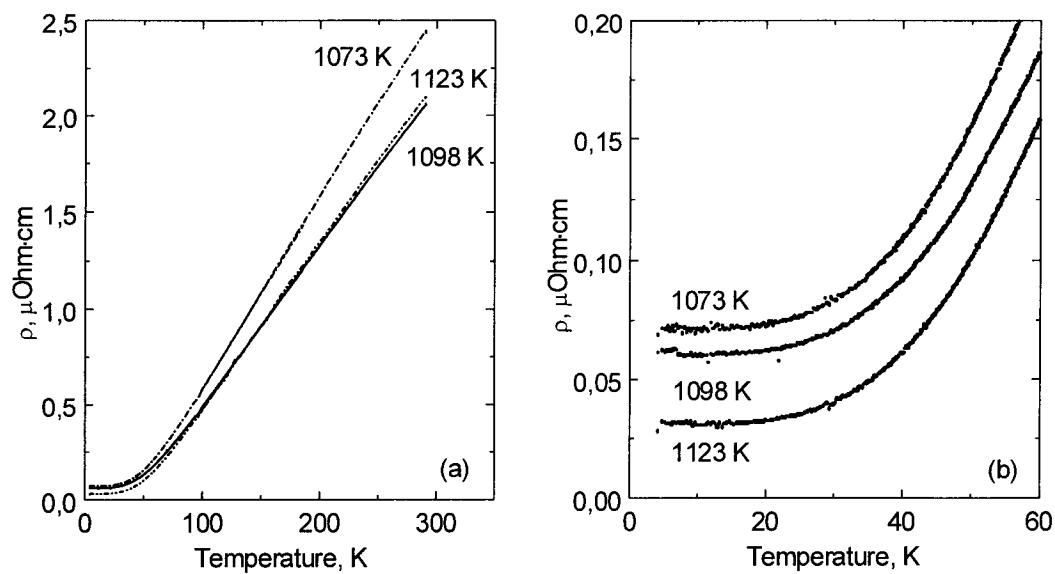


Fig. 2. Temperature dependence of the resistivity  $\rho$  of the Cu – 75 at. ppm Bi polycrystals annealed at various temperatures ( $T_{an} = 1073, 1098$  and  $1123$  K) and subsequently quenched. (a) Plots for the measurement of the temperature derivative of the resistivity  $d\rho/dT$  between 150 and 300 K. (b) Plots for the measurement of the residual resistivity  $\rho_0$  at  $T = 4.2$  K.

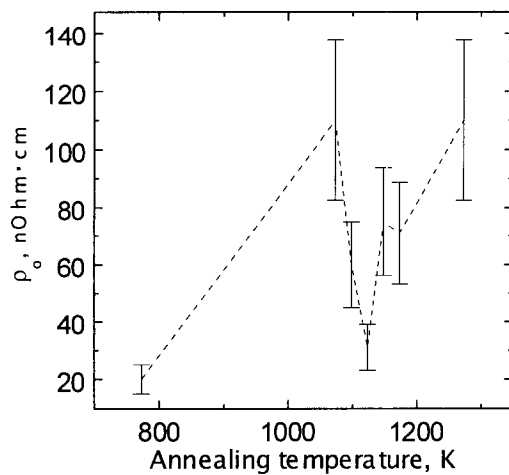


Fig. 3. Dependence of the residual resistivity  $\rho_0$  of the Cu – 75 at. ppm Bi polycrystals on the annealing temperature.

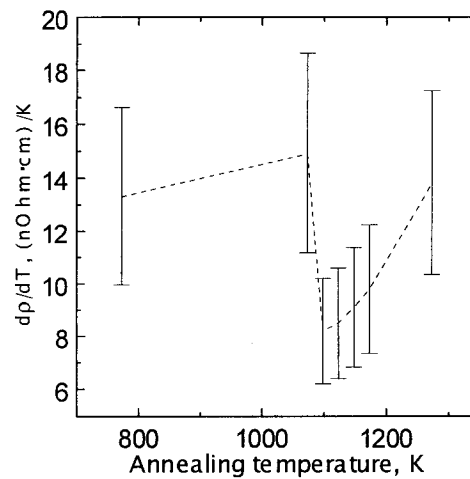


Fig. 4. Dependence of the temperature derivative of the resistivity  $d\rho/dT$  of the Cu – 75 at. ppm Bi polycrystals on the annealing temperature.

$\rho_0$  (measured at  $T = 4.2$  K, Fig. 2b) and the temperature derivative of the resistivity  $d\rho/dT$  (measured between 150 and 300 K, Fig. 2a). Values of  $\rho_0$  and  $d\rho/dT$  for the Cu – 75 at. ppm Bi polycrystals annealed at various temperatures  $T_{an}$  are presented in Figs. 3 and 4 respectively. These curves are non-monotonous. Each of them can be divided into three parts.

Residual resistivity  $\rho_0$ :

- (I) Between 773 K and 1073 K  $\rho_0$  increases from 20 to 100 nOhm-cm.
- (II) At 1073 K  $\rho_0$  drops suddenly reaching the minimum of 30 nOhm-cm at 1123 K (see also Fig. 2b).
- (III) Above 1123 K  $\rho_0$  increases to 110 nOhm-cm at 1273 K.

The temperature derivative of the resistivity  $d\rho/dT$ :

- (I)  $d\rho/dT$  increases only slightly from 13 to 14 nOhm-cm/K between 773 and 1072 K.
- (II) Sudden decrease of  $d\rho/dT$  proceeds between 1073 and 1098 K and is more pronounced in comparison with that of  $\rho_0$  (Fig. 2).
- (III) Above 1098 K  $d\rho/dT$  increases monotonously from 8 to 14 nOhm-cm/K.

### Discussion

The GB segregation of Bi in Cu was thoroughly studied in [24, 25]. Three types of behaviour for  $Z^\Phi(T)$  was observed:

- $x_{Bi}^v < 75$  at. ppm Bi. The Bi content at the GBs decreases discontinuously during the increase of temperature. At low temperatures, the Gibbsian excess of Bi atoms is approximately 2 ML, decreasing stepwise to the value of 1–1.5 ML at some definite temperature which depends on the Bi concentration in the bulk. Fig. 1 represents this behaviour.
- 75 at. ppm Bi  $< x_{Bi}^v < 120$  at. ppm Bi. The discontinuous decrease of the Bi content at the GBs during the increase of temperature is accompanied by an increase of the Bi content at the GBs at higher temperatures close to the melting point of Cu. It was the first experimental observation of an increase of the GB Gibbsian excess of the segregating impurity with an increase of the temperature in a binary system [24, 25].
- $x_{Bi}^v > 120$  at. ppm Bi. The Bi content at the GBs is approximately constant (2 ML) and does not depend on the temperature.

It was shown [24] that the classical Fowler adsorption isotherm fails to describe the GB behavior in the Cu–Bi system. Therefore, the new model of the GB prewetting phase transition was developed in [24]. From the first glance it would be natural to assume that at the GB solidus line the ordered GB core is replaced by a homogeneous layer of the quasi-liquid phase, in the spirit of the Kikuchi-Cahn model [28]. This description meets, however, serious quantitative difficulties. At high temperatures, the concentration of Bi in the Cu–Bi liquid is low, and one needs to assign a large thickness to the layer of the quasi-liquid phase in order to get the observed value of the GB Gibbsian excess  $Z^\Phi$  of Bi of 1 ML and more (see Fig. 4b). Such a thick (more than 100 interatomic distances thick) layer of a quasi-liquid cannot be stabilized by short-range forces from two solid/liquid interfaces and is, therefore, unstable.

In the prewetting model of the GB segregation we assume that the quasi-liquid layer at the GB is thin but inhomogeneous, the Bi-rich core region still having a structure similar to the structure of the untransformed GB core, but being surrounded by two thin layers of a quasi-liquid phase (Fig. 5). Indeed, a thin layer of a quasi-liquid should be strongly modulated by the adjacent crystals [29], and the structure of the GB core region may be similar to that of the untransformed GB. The driving force for the formation of two quasi-liquid layers surrounding the GB core is the high chemical energy  $\Delta G_{chem}$  associated with a stepwise change of the Bi concentration at the GB core. According to Lee and Aaronson [30]

$$\Delta G_{chem} = (x_{Bi}^{\Phi_S} - x_{Bi}^{(Cu)})^2 n_s Z_v \left( \varepsilon_{Cu-Bi} - \frac{\varepsilon_{Cu-Cu} + \varepsilon_{Bi-Bi}}{2} \right) = (x_{Bi}^{\Phi_S} - x_{Bi}^{(Cu)})^2 \Omega^I \quad (1)$$

where  $x_{Bi}^{\Phi_S}$ ,  $x_{Bi}^{(Cu)}$ ,  $n_s$  and  $Z_v$  are the Bi concentration in the GB core and in the bulk, the number of atoms per unit area of the GB core and the coordination number across the GB core, respectively.  $\varepsilon_{A-B}$  is the energy of the atomic A-B bond and  $\Omega^I$  defined by Eq. (1) is the interaction energy across the GB core. The chemical energy is associated with the presence of Cu-Bi bonds across the GB core, which are energetically unfavorable in systems with a high positive enthalpy of mixing. It is this mixing enthalpy which causes the retrograde solubility in the bulk [31, 32].

This approach permitted to describe quantitatively the observed breaks on the  $Z^\Phi(T)$  dependence and to construct the line of the GB premelting phase transition in the Cu-Bi bulk phase diagram. This phase diagram is shown in the Fig. 6. The bulk solidus (thick line) was experimentally obtained in [31]. The GB solidus (thin line) was calculated basing on the experimental data on Bi segregation in polycrystals [24, 25]. The GB solidus represent the GB prewetting phase transition and is completely positioned in the solid solution field of the bulk phase diagram. In Fig. 6 the schemes of the microstructures are also given for three main fields of the phase diagram. At the low concentrations of Bi only the (Cu) phase (Cu-based solid solution) exists in the bulk. The conventional segregation of Bi  $\Phi_S$  is present in the GBs, it means the GBs remain "solid". At the thin retrograde line the GB prewetting phase transition occurs. Between the thin retrograde line (GB solidus) and thick one (bulk solidus) only the solid solution (Cu) is present in the bulk, but GBs contain now the (prewetting) GB phase  $\Phi_L$ . In other words, the bulk remains solid, but the GBs became "liquid". In the two-phase area of the bulk diagram the bulk liquid phase  $L$  appears in addition to the (Cu) solid solution. The GBs conserve the same structure  $\Phi_L$ . It is important that the GB liquid-like phase appears at the GB solidus line. The GB state does not change principally at the bulk liquidus line when the "true" liquid phase appear in the system.

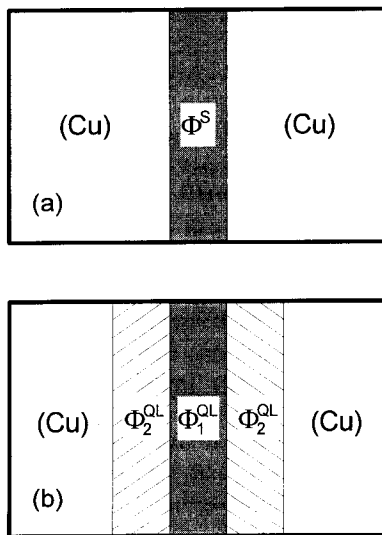


Fig. 5. Two possible GB structures: (a) GB with a Bi-enriched solid core and (b) prewetted GB. QL = quasi-liquid.

In this work, together with GB segregation measurements, the data on resistivity of the Cu – 75 at. ppm Bi polycrystals were experimentally obtained (Figs 2 to 4). By comparing of Figs 1, 3 and 4 it can be clearly seen that the values of  $\rho_0$  and  $d\rho/dT$  measured, respectively, at 4.2 K and between 150 and 300 K are very sensitive to the state of GBs array in the the Cu(Bi) polycrystals. Namely, the sudden decrease of  $\rho_0$  and  $d\rho/dT$  is observed which is very similar to that of  $Z^\Phi$ . The data on the temperature dependence of  $\rho_0$ ,  $d\rho/dT$  and  $Z^\Phi$  for the Cu – 75 at. ppm Bi polycrystals are compared in the Fig. 6. The filled and open symbols for  $\rho_0$  and  $d\rho/dT$  have the same meaning as for  $Z^\Phi$ , namely the filled symbols depict the values of  $\rho_0$ ,  $d\rho/dT$  and  $Z^\Phi$  before their sudden decrease. The open symbols depict the values above the temperature of the sudden drop of  $\rho_0$ ,  $d\rho/dT$  and  $Z^\Phi$ . It can be seen from the Fig. 6 that the temperatures of the sudden decrease of  $\rho_0$  and  $d\rho/dT$  coincide pretty well with that of  $Z^\Phi$ . The GB solidus shown in Fig. 6 was obtained in [24–26] on polycrystals. By the brittle GB failure of a polycrystal

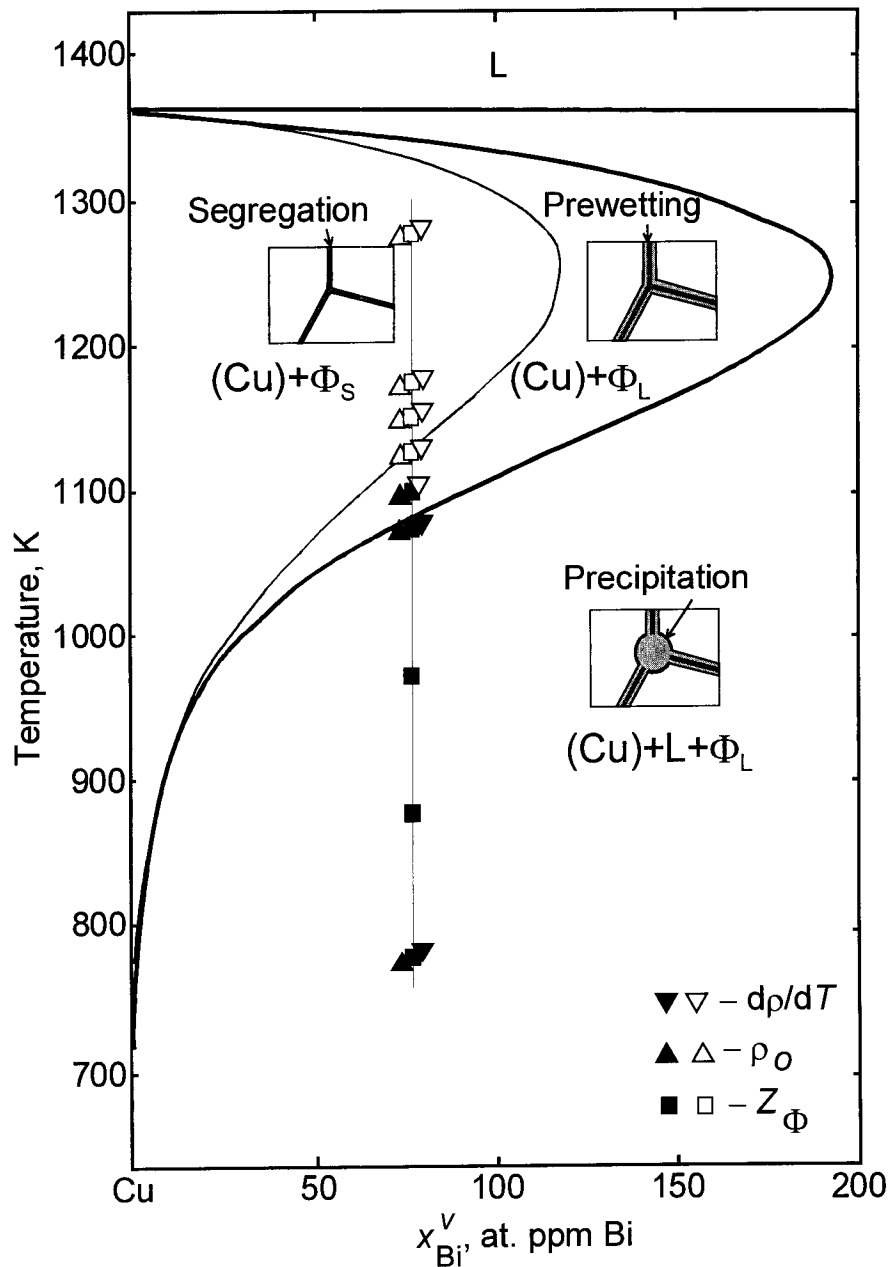


Fig. 6. Cu-Bi phase diagram showing the lines of bulk solidus experimentally obtained in [31] and GB solidus for Cu-Bi polycrystals calculated in [24] basing on the GB segregation data measured in [25]. Schemes of the microstructure in various fields of the diagram are shown:  $(Cu)+\Phi_S$ : solid solution in the bulk and segregation in the GBs.  $(Cu)+\Phi_L$ : solid solution in the bulk and a quasi-liquid layer in the GBs.  $(Cu)+L+\Phi_L$ : solid solution and melt phases in the bulk and a quasi-liquid layer in the GBs. The experimental points for residual resistivity  $\rho_0$  and derivative of the resistivity  $d\rho/dT$  measured at 75 at. ppm Bi are shown together with GB segregation data. The transition from the open to solid symbols represents the GB prewetting phase transition.

(1) enough brittle GBs have to be present in the polycrystal and (2) the "weakest" GBs are broken. Therefore, the GB solidus obtained with the aid of AES measurements of GB segregation on the failure surface is resulted from the averaging of GB segregation data on several GBs. For each value of Bi concentration  $x_{Bi}^v$  and  $T$  the set of GBs is different. The GB solidus lines for individual GBs differ both from each other and from solidus obtained for polycrystals [32]. During the the measurements of resistivity all GBs present in the polycrystal contribute together with the Cu(Bi) bulk to the values of  $\rho$ ,  $\rho_0$  and  $d\rho/dT$ .

Let us try to explain the influence of the microstructure of the Cu–Bi polycrystals on the behaviour of  $\rho_0$  and  $d\rho/dT$ . The electric conductivity of the metals like aluminium or copper is very sensitive to the presence of the crystal defects having the dimensions comparable with the wavelength of the electron on the Fermi surface [33]. In case of copper alloyed with bismuth the valency and ionic radii of Cu and Bi are very different. Therefore, the electron scattering on the atoms of alloying element has to determine the electric conductivity of the Cu–Bi alloys. This scattering has to influence mainly the residual resistivity  $\rho_0 = \rho(T \rightarrow 0)$  of the Cu–Bi alloys. Close to the GBs, the concentration of Bi is higher than that in the bulk. The presence of Bi has to influence essentially both the value of  $\rho$  and its temperature dependence  $\rho(T)$  for the Cu–Bi polycrystals. The influence of Bi on  $\rho$  and  $\rho(T)$  for the Bi-rich alloys is due to the low concentration of charge carriers in Bi (about  $10^{-5}$  per atom in the pure metallic Bi) and due to the high distortions of crystal structure of Cu in the GBs and close to GBs. In order to characterize the dependence  $\rho(T)$  the temperature derivative of the resistivity  $d\rho/dT$  was detected on the slope of the linear parts of  $\rho(T)$  plots (Fig. 2a). The linear behaviour of the temperature dependence  $\rho(T)$  is typical for the metallic alloys for  $T > 0.5 \theta_D$  ( $\theta_D$  being the Debye temperature).  $\theta_D$  for copper is 333 K [33]. Fig. 2 reveals that this law is valid also for diluted Cu–Bi alloys. Namely, the linear behaviour of  $\rho(T)$  is observed above 150 K.

Both  $\rho_0$  and  $d\rho/dT$  (Figs. 3 and 4) are very sensitive to the intersection of GB solidus line (Fig. 6). As a result, both  $\rho_0$  and  $d\rho/dT$  values decrease suddenly for the samples annealed close to the GB solidus. Afterwards,  $\rho_0$  and  $d\rho/dT$  increase for the samples annealed at higher temperatures and reach the "starting" values at  $T_{an} = 1273$  K. Let us analyze the behaviour of  $\rho_0$  and  $d\rho/dT$  in three temperature regions mentioned above. In the region I (773 to 1073 K) the values of  $\rho_0$  and  $d\rho/dT$  increase nearly linear with increasing temperature. By increase of the annealing temperature from 773 to 1073 K the solubility of Bi in the bulk increases about 10 times (Fig. 6, [31]). Therefore, the equilibrium concentration of Bi in the bulk increases with increasing  $T_{an}$  up to the intersection of  $x_{Bi}^v = 75$  at. ppm Bi line and remains constant at higher  $T_{an}$ . The increase of the number of scattering centers (e.g. Bi atoms) in the bulk solid solution leads to the increase of both  $\rho_0$  and  $d\rho/dT$ . Here, the value of  $\rho_0$  increases about 5 times, but  $d\rho/dT$  increases only slightly. This behaviour can be perfectly explained by the theoretical calculations of the resistivity of the metal containing the solute atoms performed in the "classical" temperature limit [34]. Therefore, the behaviour of  $\rho_0$  and  $d\rho/dT$  in the temperature region I can be easily explained without additional considerations on the microstructure of GB regions.

In order to explain the drastic changes of  $\rho_0$  and  $d\rho/dT$  in the regions II and III (Figs. 3 and 4), the possible changes of the microstructure of GBs and GB regions has to be considered. Indeed, the essential change of  $d\rho/dT$  (1.5 to 2 times) can only proceed due to the formation of the layer of new phase on the GBs. This new GB phase has to contain the large amount of Bi leading to the distortion of the crystallographic structure and, therefore, to the essential dispersion of bond lengths and angles. The volume of this phase has to be not negligible, and its effective thickness has to be comparable with the medium range order length [34]. Such hypothesis correlates with the idea of formation of the GB prewetting layer proposed earlier [24–26, 32]. However, in order to explain the essential change of  $d\rho/dT$  (1.5 to 2 times) we have to suppose that each of the quasi-liquid layers  $QL_2+QL_1+QL_2$  shown in the scheme Fig. 5 possesses the thickness of about 10 interatomic distances, and the overall thickness of the GB phase is about 10 nm. In the framework of such an



approach it is possible to explain the similar behaviour of  $\rho_0$ ,  $dp/dT$  and  $Z^\Phi$  in the temperature regions II and III by the essential change of the GB properties, namely by the change of the Bi concentration profile and dispersion of the bond lengths and angles. It can be supposed that in the region II (where  $\rho_0$ ,  $dp/dT$  and  $Z^\Phi$  decrease drastically) the central layer  $QL_1$  (Fig. 5) becomes thinner and disappears. In the region III the number of Bi atoms on the GB decreases with increasing temperature according to the conventional GB adsorption laws, and the GB profile of Bi concentration becomes broader.

Therefore, the combination of AES measurements of GB segregation and of the low-temperature resistivity of polycrystals is very informative and permits one to detect the GB phase transitions, particularly the GB prewetting phase transition. The investigation of the GB phase transitions with the aid of the GB segregation measurements needs the GB fracture and, therefore, is restricted by the systems possessing the GB brittleness. Measurements of  $\rho_0$  and  $dp/dT$  can be performed for all polycrystals including the ductile ones. Therefore, this method can be very effective for the search and investigation of the GB phase transitions.

In the prewetting model of the GB segregation we assume that the quasi-liquid layer  $\Phi_L$  at the GB is thin but inhomogeneous. The Bi-rich core still has a structure similar to the structure of the untransformed GB core, but being surrounded by two thin layers of the quasi-liquid phase (Figs. 5 and 6) [25]. The presence of the quasi-liquid layer  $\Phi_L$  at the GBs can explain the enhanced diffusivity in the Cu–Bi system [35, 36], similar to that observed earlier in the Fe–Si–Zn system [15–18]. At higher concentrations of Bi, after intersection of the bulk solidus line the bulk liquid L appears in the material together with solid solution (Cu) and a quasi-liquid phase  $\Phi_L$  at the GBs. At lower concentrations of Bi, after intersection of the GB solidus line only the solid solution (Cu) is present in the material, containing GBs with a conventional segregation layer  $\Phi_S$ . Therefore, the GB prewetting and wetting phase transitions can lead to the anomalous high diffusion permeability of polycrystals due to the presence of high-diffusivity GB paths containing the liquid or quasi-liquid layers [15–18, 35, 36]. Other kinetic processes, like GB mobility or grain growth can also be accelerated due to the presence of the liquid or quasi-liquid layers in GBs [14, 23]. Therefore, the investigation and construction of the GB phase diagrams is very important for the prediction of properties of fine-grained polycrystals and nanocrystalline materials.

### Acknowledgements

Prof. S. Hofmann, Prof. E. Rabkin, Prof. Mittemeijer and Dr. L.-S. Chang are acknowledged for the fruitful discussions. The financial support of the INTAS Programme (contract 99-1216), Deutsche Forschungsgemeinschaft (contracts Gu 258/12-1 and BA-1768/1-2), Russian Foundation of Basic Research and Copernicus network (contract ERB IC15 CT98 0812) is acknowledged.

### References

- [1] S. Dietrich, in: *Phase Transitions and Critical Phenomena*, edited by C. Domb and J. H. Lebowitz (Academic, London, 1988) 12, p. 2.
- [2] D. Jasnov, *Rep. Prog. Phys.* 47 (1984), p. 1059.
- [3] G. de Gennes, *Rev. Mod. Phys.* 57 (1985), p. 827.
- [4] E.L. Maksimova, E.I. Rabkin, L.S. Shvindlerman and B. B. Straumal, *Acta metall.* 37 (1989), p. 1995.
- [5] B.B. Straumal and L.S. Shvindlerman, *Acta metall.* 33 (1985), p. 1735.
- [6] E.L. Maksimova, L.S. Shvindlerman and B.B. Straumal, *Acta metall.* 36 (1988), p. 1573.
- [7] E.L. Maksimova, L.S. Shvindlerman and B.B. Straumal, *Acta metall.* 37 (1989), p. 2855.
- [8] T.G. Ference and R.W. Balluffi, *Script. metall.* 22 (1988), p. 1929.
- [9] F. Ernst, M.W. Finnis, A. Koch, C. Schmidt, B. Straumal and W. Gust, *Z. Metallk.* 87 (1996), p. 911.

- 
- [10] B. Straumal, T. Muschik, W. Gust and B. Predel, *Acta metall. mater.* 40 (1992), p. 939.
- [11] B. Straumal, W. Gust and D. Molodov, *Interface Sci.* 3 (1995), p. 127.
- [12] B.B. Straumal, W. Gust and T. Watanabe, *Mater. Sci. Forum* 294–296 (1999), p. 411.
- [13] B. Straumal, D. Molodov and W. Gust, *Mater. Sci. Forum* 207–209 (1996), p. 437.
- [14] B. Straumal, S. Risser, V. Sursaeva, B. Chenal and W. Gust, *J. Physique IV* 5-C7 (1995), p. 233.
- [15] E.I. Rabkin, V.N. Semenov, L.S. Shvindlerman and B.B. Straumal, *Acta metall. mater.* 39 (1991), p. 627.
- [16] O.I. Noskovich, E.I. Rabkin, V.N. Semenov, L.S. Shvindlerman and B.B. Straumal, *Acta metall. mater.* 39 (1991), p. 3091.
- [17] B.B. Straumal, O.I. Noskovich, V.N. Semenov, L.S. Shvindlerman, W. Gust and B. Predel, *Acta metall. mater.* 40 (1992), p. 795.
- [18] B. Straumal, E. Rabkin, W. Lojkowski, W. Gust and L.S. Shvindlerman, *Acta mater.* 45 (1997), p. 1931.
- [19] E.I. Rabkin, B.B. Straumal and L.S. Shvindlerman, *Int. J. Mod. Phys. B* 5 (1991), p. 2989.
- [20] R.H. French, H. Müllejans, D.J. Jones, G. Duscher, R.M. Cannon, and M. Rühle, *Acta mater.* 46 (1998), p. 2271 and references therein.
- [21] E.I. Rabkin, L.S. Shvindlerman and B.B. Straumal, *J. Less-Common Met.* 158 (1990), p. 23.
- [22] E.I. Rabkin, L.S. Shvindlerman and B.B. Straumal, *J. Less-Common Met.* 159 (1990), p. 43.
- [23] D.A. Molodov, U. Czubayko, G. Gottstein, L.S. Shvindlerman, B.B. Straumal and W. Gust, *Phil. Mag. Lett.* 72 (1995), p. 361.
- [24] L.-S. Chang, E. Rabkin, B.B. Straumal, S. Hofmann, B. Baretzky and W. Gust, *Defect Diff. Forum* 156 (1998), p. 135.
- [25] L.-S. Chang, E. Rabkin, B. B. Straumal, B. Baretzky and W. Gust, *Acta mater.* 47 (1999), p. 4041.
- [26] L.-S. Chang, E. Rabkin, B. Straumal, P. Lejcek, S. Hofmann and W. Gust, *Scripta mater.* 37 (1997), p. 729.
- [27] L.-S. Chang: *Ph.D. Thesis* (University of Stuttgart, Germany, 1998).
- [28] R. Kikuchi and J.W. Cahn, *Phys. Rev. B* 36 (1987), p. 418.
- [29] J. Howe, *Phil. Mag. A* 74 (1996), p. 761.
- [30] Y.W. Lee and H.I. Aaronson, *Acta metall.* 28 (1980), p. 539.
- [31] L.-S. Chang, B.B. Straumal, E. Rabkin, W. Gust and F. Sommer, *J. Phase Equilibria* 18 (1997), p. 128.
- [32] B. Straumal, S.I. Prokofjev, L.-S. Chang, N.E. Sluchanko, B. Baretzky and W. Gust, *Defect Diff. Forum* (2001) in press.
- [33] J. Friedel: *Dislocations* (Pergamon Press, London, 1964)
- [34] A.P. Zhernov, N.A. Chernoplekov and E. Mrozan: *Metals with non-magnetic impurities* (Energoatomizdat, Moscow, 1992) in Russian.
- [35] B. Joseph, F. Barbier and M. Aucouturier, *Mater. Sci. Forum* 294–296 (1999), p. 735.
- [36] B. Joseph, F. Barbier, G. Dagoury and M. Aucouturier, *Scripta Mater.* 39 (1998), p. 775.